J Mater Sci (2008) 43:4079–4090
DOI 10.1007/s10853-007-2315-1

REES RAWLINGS FESTSCHRIFT

Service life prediction for refractory materials

D. N. Boccaccini · M. Cannio · T. D. Volkov-Husoviæ · E. Kamseu · M. Romagnoli · P. Veronesi · C. Leonelli · I. Dlouhy · A. R. Boccaccini

Received: 14 June 2007 / Accepted: 13 November 2007 / Published online: 3 April 2008

Abstract Ultrasonic pulse velocity testing and image analysis were used to predict the thermal stability of cordierite–mullite refractories. Two compositions used as substrates in fast firing of porcelain whiteware, characterized by different microstructure and crack propagation behavior, were investigated. Fracture strength and fracture toughness values were obtained from three point bending test and chevron notched specimen technique, respectively. The measurement of the ultrasonic velocity was used to assess the material degradation with increasing number of thermal-shock cycles and specimen damage was monitored using image analysis to obtain further evidence of material degradation. The correlation between thermo-mechanical properties, ultrasonic velocity, microstructure, crack-propagation behavior and thermal-shock resistance was discussed. A remarkable similarity was found between the variation of ultrasonic velocity (when measured through the length of the refractory plates) and fracture strength with number of thermal shock cycles. On the other hand, the development of surface microcracking, as monitored by image analysis, is in good agreement with the variation of K_{IC} with the number of thermal-shock cycles. The variation of the $\frac{d\sigma_f}{dE_{dyn}}$ ratio with number of thermal-shock cycles shows the highest gradient of the investigated trends and it is proposed as a promising parameter to differentiate refractory materials regarding their different thermal shock behavior. Service life prediction models for refractory plates, from measured values of ultrasonic velocity and surface damage analysis, were proposed and validated.

D. N. Boccaccini (✉) · M. Cannio · E. Kamseu · M. Romagnoli · P. Veronesi · C. Leonelli
Dipartimento di Ingegneria dei Materiali e dell'Ambiente, Università di Modena e Reggio Emilia, Via Vignolese 905, 41100 Modena, Italy
e-mail: boccaccini.dino@unimore.it

T. D. Volkov-Husoviæ
Faculty of Technology and Metallurgy, University of Belgrad, Karnegijeva 4, 11120 Belgrade, Serbia and Montenegro

I. Dlouhy
Institute of Physics of Materials, ASCR, 61662 Brno, Czech Republic

A. R. Boccaccini
Department of Materials, Imperial College London, London SW7 2BP, UK

Introduction

The characterization of thermal-shock degradation of commercial refractories in service is of prime concern to industries involving high-temperature processes. When refractory materials are subjected to industrial thermal cycles crack initiation and/or propagation occurs resulting in loss of stiffness, mechanical strength, and overall material degradation. The practical and economic effects of thermal-shock damage on refractories are reflected in the ever increasing number of research projects devoted to improve the thermal-shock resistance of refractory materials [1–3]. Early investigations of thermal-shock behavior of ceramics were performed by Norton [4], Goodrich [5] and Hasselman [6, 7]. Hasselman put forward a theoretical framework for establishing criteria for crack propagation due to thermal shock. Nakayama [8] introduced the work of fracture (WOF) concept that enabled a fracture mechanics approach to be used in conjunction with Hasselman's thermal-shock parameters. Experimental evidence to support Hasselman's thermal-shock resistance parameters was

provided initially by Davidge and Tappin [9] for dense alumina. In another early study, Tacrarian [10] reported that the strength after thermal shock of insulating refractories decreased continuously with increasing temperature. In subsequent years, measurement of fracture strength and Young's modulus of components after thermal shock have become popular characterization methods of thermal-shock damage.

The testing of refractories has involved historically mostly destructive test methods for both room and high-temperature characterization. Such testing, if conducted on a statistically representative sample population, results in a large number of specimens being destroyed. The thermal-shock evaluation by destructive tests is prescribed by two active standards:

(i) The ASTM C1171-05 "Standard Test Method for Quantitatively Measuring the Effect of Thermal Shock and Thermal Cycling on Refractories".
(ii) The document CEN_TS 993-11:2002 "Determination of thermal stability", issued by the Technical Committee TC-187 "Refractory materials and products" of the European Committee for Standardization where two methods are proposed: method A) for refractory components and method B) specifically for unshaped refractory castables.

The development and use of higher quality raw materials have increased the cost of refractories and led to consider the use of non-destructive testing methods for characterizing thermal-shock damage. Of all the various available non-destructive test methods, the ultrasonic pulse velocity technique has attracted a lot of interest [11]. Initial use of sonic velocity was dedicated to specialized applications such as fireclay coke oven shapes [12], but from the 1980s it has been applied to bulk refractories as well [W. Miller, Unpublished Paper, 13]. Currently, the relevant ASTM standard is C1419-99a "Standard Test Method for Sonic Velocity in Refractory Materials at Room Temperature and Its Use in Obtaining an Approximate Young's Modulus". Semi-empirical equations have been proposed to correlate the ultrasonic velocity or Young's modulus to the strength or porosity of various refractories [14, 15]. Another important method for assessing damage of materials non-destructively is image analysis of the specimen surface damage. Recent work by Volkok-Husoviæ [16], for example, has focused on the use of image analysis to examine fracture strength and modulus of elasticity changes by monitoring the development of surface damage in alumina-based refractory materials. From those studies, image analysis emerges as a promising non-destructive method for thermal shock damage characterization and to pin point useful semi-empirical mathematical models for service life prediction of refractory compounds.

The aim of this work was to study the degradation of commercially available cordierite–mullite refractory materials subjected to industrial thermal cycles by both destructive and non-destructive characterization. Degradation curves obtained from non-destructive testing methods (e.g., ultrasonic velocity testing (UPVT) and image analysis), were for the first time compared with those obtained from fracture strength and fracture toughness measurement carried out by three point bending test and chevron notched technique, respectively.

Experimental

Material

Two series of commercially available refractory plates of cordierite–mullite composition, hereafter indicated as RSE and BRT, were investigated. These refractory plates are widely used as supports in whiteware fast firing cycles [17]. Thus the thermal-shock cycles considered in this investigation correspond to the industrial thermal treatment used for the firing of porcelain articles, which involve heating to $T = 1{,}275$ °C at 15 °C/min and cooling rate of 15 °C/min. The materials have been tested previously on-duty in industrial kilns and they appear to exhibit different thermal-shock failure mechanisms: one material (RSE) being characterized by early crack initiation and slow crack propagation, whilst the second material (BRT) exhibiting delayed crack initiation and fast fracture propagation [17]. Scanning electron microscopy (SEM) has been performed on polished sections of samples after gold coating to characterize the microstructure of the as-received materials in previous investigations [17, 18]. Figure 1a, b shows the typical microstructure of the materials for samples in the as-received state while Fig. 1c, d shows the microstructure of samples after 110 industrial thermal-shock cycles. The chemical analysis of the materials investigated is reported in Table 1 while Table 2 shows the basic properties of these materials, in the as-received condition, measured at room temperature in a previous work [18]. From a compositional point of view, BRT material presents higher amount of SiO_2 and alkali content while lower Al_2O_3 content, as evidenced in Table 1. The chemical composition plays a major role in the characteristics of the aggregate–matrix bond interface, which determines the main thermo-mechanical properties of refractory materials, i.e., thermal shock resistance. Table 2 confirms that RSE material is denser than BRT and this could explain its higher flexural strength at room temperature. However, the fracture toughness of RSE is lower than that of BRT.

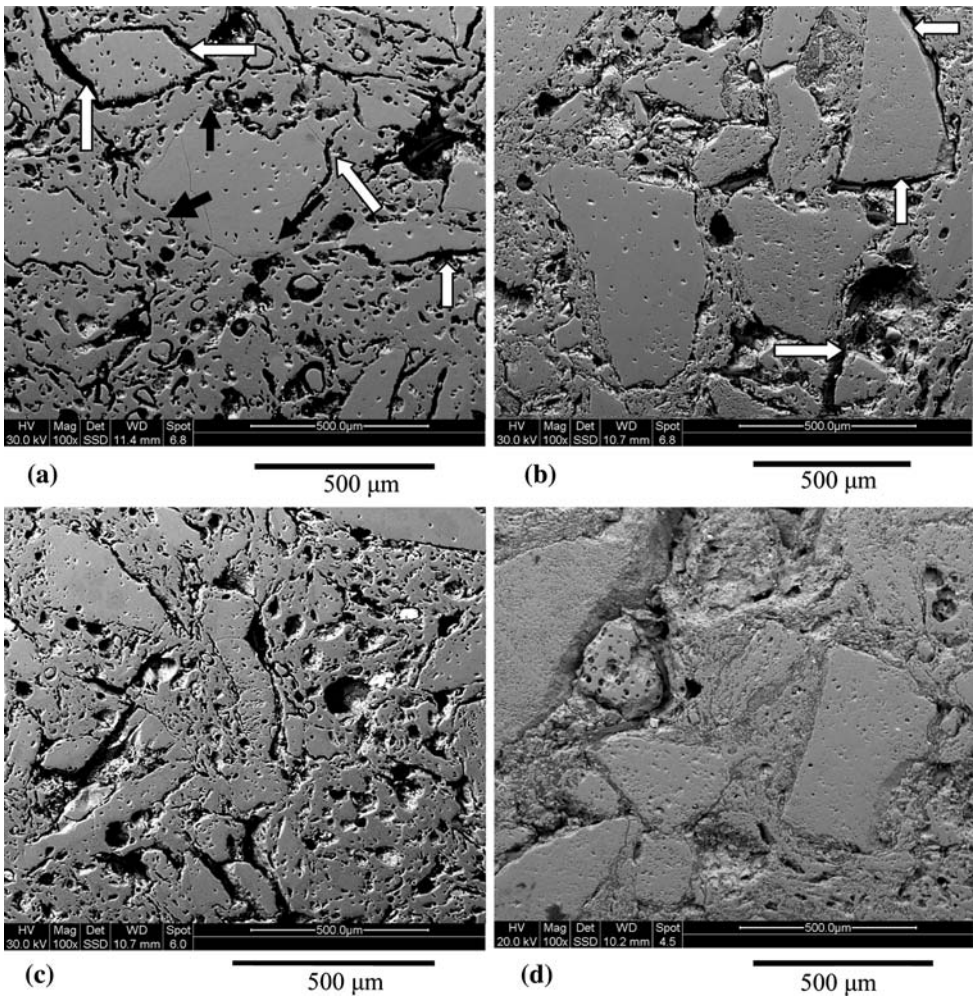

Fig. 1 SEM micrographs showing the microstructure of as-received refractory plates for (**a**) BRT and (**b**) RSE samples (white arrows indicate microcracking while black arrows crack bridges); the images (**c**, **d**) show the microstructure after 110 industrial thermal cycles for (**c**) BRT and (**d**) RSE samples

Table 1 Chemical composition of the two refractory samples investigated (RSE and BRT) (in wt%)

Oxide	wt%	
	RSE	BRT
SiO_2	43.14	46.42
Al_2O_3	45.51	41.51
CaO	0.59	0.74
MgO	8.09	8.32
Na_2O	0.05	0.12
K_2O	0.51	0.64
Fe_2O_3	1.55	1.52
TiO_2	0.57	0.71
Total	100.00	100.00

Table 2 Physical, thermal and mechanical properties of the as-received RSE and BRT refractory materials

Parameter	RSE	BRT
Bulk density, $\rho(\mathrm{g/cm^3})$[a]	2.08	1.91
Thermal expansion coefficient, $\alpha\,(25{-}1,250^{\circ}\mathrm{C})(^{\circ}\mathrm{C}^{-1}\times 10^{-6})$	3.06×10^{-6}	2.49×10^{-6}
Apparent porosity (%)	24	28
Dynamic Young's modulus, E_{dyn}, Impulse Excitation Technique (I.E.T.), (GPa)	21.5	15.7
Dynamic Poisson's ratio, μ_{dyn} Impulse Excitation Technique (I.E.T.)	0.16	0.16
Three point bending strength, σ (MPa)	22	18
Fracture toughness, K_{IC} ($\mathrm{MPam^{1/2}}$)	0.35	0.40

[a] GeoPyc 1360 Micromeritics, Norcross, GA 30093-1877, USA (reproducibility ±1.1%)

Destructive testing

Three point bending strength

Fracture strength data were determined at room temperature before and after 110, 360, and 510 industrial thermal cycles. The prismatic bars of dimensions $80\times25\times5$ $\mathrm{mm^3}$ used for these measurements were cut from the refractory plates using a diamond saw. Tests were carried out in three-point

bending configuration with a 70 mm span and a cross-head speed of 3 mm/min using a universal testing machine (MTS 810, USA). At least 10 samples for each condition were tested and the results were averaged. The fracture strength was calculated by using the following equation:

$$\sigma_f = \frac{3PL}{2BW^2} \quad (1)$$

where P is the maximum load, L the span, B the width of the specimens and W their thickness.

Fracture toughness determination

Fracture toughness data of selected samples before and after industrial thermal cycles were obtained by the chevron notch (CN) technique at room temperature. The specimen geometry employed in this test was a bar with nominal cross-section dimensions of $W = 4$ mm, $B = 3$ mm. Chevron notches with angles of 90° were cut using a thin diamond wheel. The specimens were loaded in three-point bending configuration with span 16 mm at a constant cross-head speed of 0.01 mm/min. The samples were about 30 mm long thus it was possible to obtain two fracture toughness values from each bar (two chevron notches per bar). Graphs of load versus deflection were recorded and the fracture toughness was calculated from the maximum load (F_{max}) and the corresponding minimum value of geometrical compliance function (Y^*_{min}) using the following equation [19]:

$$K_{IC} = \frac{F_{max}}{BW^{1/2}} Y^*_{min} \quad (2)$$

where B and W are the width and thickness of the specimens, respectively. The calculation of the function Y^*_{min} for chevron notched bending bars was based on Bluhm's slice model [20]. The calculation procedure used for the purposes of this investigation has been described in detail elsewhere [19]. The chevron-notch depth (a_0) was measured from optical micrographs of fractured specimens.

Non-destructive testing

Ultrasonic pulse velocity testing

A commercial ultrasonic testing instrument of transmission type (PUNDIT *plus* PC1006, CNS Farnell Ltd., Hertfordshire, England) was used. The instrument consists of a pulse generator and timing circuit coupled to two transducers (220 kHz) that were positioned manually at opposite ends of each specimen. Each transducer had a 2 mm thick rubber tip to help overcome measurement problems due to the roughness of the refractory surface. The ultrasonic velocity, v, is calculated from the distance between the two transducers and the electronically measured transit time of the pulse as:

$$v\,(\text{m/s}) = \frac{d}{t} \quad (3)$$

where d = distance between the two transducers (m) and t = transit time (s).

By determining the ultrasonic velocity and bulk density (ASTM C-134) of a refractory it is possible to calculate the dynamic modulus of elasticity using the equation below (ASTM C 1419-99a):

$$E_{dyn} = v^2 \rho \left(\frac{(1 + \mu_{dyn})(1 - 2\mu_{dyn})}{1 - \mu_{dyn}} \right) \quad (4)$$

where v = pulse velocity (m/s), ρ = density (kg/m^3) and μ_{dyn} = dynamic Poisson's ratio.

Fifty refractory plates of each series with identical dimensions (520 × 340 × 12 mm^3) were investigated. For each refractory plate, measurements of ultrasonic pulse velocity through the length and thickness (hereafter indicated as v_L and v_T, respectively) on direct transmission disposition were performed. Each test was run at least five times to correctly validate the ultrasonic velocity. The measurements were performed on the same batch of refractory plates in the as-received condition and after 110, 360, and 510 industrial thermal cycles.

Image analysis

Chalk powder is employed to color the refractory surfaces to differentiate between damaged and non-damaged areas. The chalk powder used was selected between the commercially available products taking into account the powders showing the higher contrast, the lack of reactivity with the refractory specimen investigated and the price.

When the appropriate color is selected, it is possible to quantitatively measure the ratio and level of damaged and non-damaged areas by means of image analysis using a statistical approach. The area without damage is in general colored by the chalk powder in the majority of the experiments, while the damaged areas keep the basic color of the refractory materials.

This method of coloring the refractory samples depends on the bonding present between the chalk powder and the original surface of the refractories. Good quality bonding can be defined when chalk powder is on the non-damaged surface, and it could not be removed unless brush or sponge is used. If this bonding is strong enough, then chalk powder is likely on the non-damaged area of the sample. However, if the bonding is weak and the value of the damage area is

close to that of the grain diameter, the chalk powder should color the damaged area.

The IMAGE PRO PLUS program (Materials_Pro® Analyzer, Version 3.1, Media Cybernetics, Silver Spring, MD, USA) was used for image analysis. Ten different refractory plates after 0, 110, 360, and 510 industrial thermal cycles were considered and five samples were cut from each refractory plate. The specimens were covered with thin chalk-powder film before surface damage was investigated. The film provided better contrast and differentiation of damaged and non-damaged surfaces. Photographs of thermally degraded specimens were taken before and after 110, 360, and 510 industrial thermal shock cycles. At least 10 photographs per sample were analyzed to obtain a reliable characterization of the microstructure. Refractory specimen surfaces were fresh, as any additional process could damage the original state of the sample. The ratio between sample surface area (P_0) and damaged surface area (P) was calculated for each refractory material. The results of $(\frac{P_0}{P}\,\%)$ ratio against the number of thermal-shock cycles for both compositions were plotted.

Determination of thermal-shock resistance parameters R and R'''''

The classic theory on the thermal-shock resistance of brittle ceramics was established by Hasselman [6, 7]. In the theory thermal shock resistance parameters (R, R''''', etc.) were introduced to evaluate the resistance of material against crack initiation and propagation. The R parameter (°C) represents the resistance of a material to fracture initiation by very severe thermal shock and it is calculated by the following equation:

$$R(^{\circ}\mathrm{C}) = \frac{\sigma_f(1-\upsilon)}{\alpha E} \tag{5}$$

where σ_f is the fracture strength, υ is the Poisson's ratio, α is the thermal expansion coefficient, and E is Young's modulus.

For mild thermal shock, the following equation is valid:

$$R(W/m) = \frac{\lambda\sigma_f(1-\upsilon)}{\alpha E} \tag{6}$$

where λ is the thermal conductivity of the specimen. A given thermal-shock environment can be estimated mild or severe by considering the Biot number, expressed by $\beta = h^* W/\lambda$, where W is the sample thickness and h the heat transfer coefficient (the energy that enters the material per unit temperature difference between the atmosphere and the surface). If $2/\beta \gg 1$ then the thermal shock is considered mild and R' parameter should be used; if $2/\beta \ll 1$ the thermal shock is severe and R is the relevant figure of merit. Considering a heat transfer coefficient of $h = 200$ W/m^2 °C for the air cooling condition of the industrial thermal treatment [21], the specimen thickness $W = 12$ mm and the thermal conductivity of cordierite–mullite refractories $\lambda = 0.8$ W/m K (porosity $\sim$ 25%) [22]; then $2/\beta = 0.8 < 1$ and hence R can be considered the appropriate figure of merit.

The resistance of the refractory materials to thermal-shock damage by kinetic crack growth damage is calculated by the resistance parameter R'''' as follows:

$$R''''(m) = \frac{K_{IC}^2}{\sigma f^2(1-\upsilon)} \tag{7}$$

where K_{IC} is the fracture toughness.

For refractory manufacturers and users, it is important to find reliable techniques and parameters to assess, after few representative thermal-shock cycles, which material or which composition should behave better when submitted to real thermal-shock-service-life conditions. According to the Hasselman's theory, the resistance to thermal-shock damage in refractory materials can be also assessed by the relationship between retained fracture strength and original fracture strength [23], described as:

$$\frac{\sigma_r}{\sigma_o} \approx R'''' \tag{8}$$

where σ_r = retained strength, σ_o = fracture strength before thermal shock.

In this work, the retained property ratios of the thermo-mechanical properties, measured after 110 industrial cycles, were determined. In the next section we discuss which parameter, after few thermal shock cycles, could reliably forecast the service life of the refractory plates when submitted to on-duty thermal-shock conditions.

Results and discussion

Fracture strength-ultrasonic velocity correlation

Refractory materials inevitably contain some flaws in the form of porosity, microcracks and impurities. When ceramics containing inherent flaws are subjected to severe thermal shock, damage concentrated at tips of those pre-existing flaws will be generated leading to higher number of microcracks and hence the fracture strength will be degraded. The change in strength as a function of the cumulative number of thermal-shock cycles is presumably due to the accumulation and coalescence of thermal-shock-induced micro-crack damage [24].

Figure 2 shows the effects of the industrial thermal-shock cycles on fracture strength and ultrasonic velocity, measured through the length (v_L), of the refractory plates.

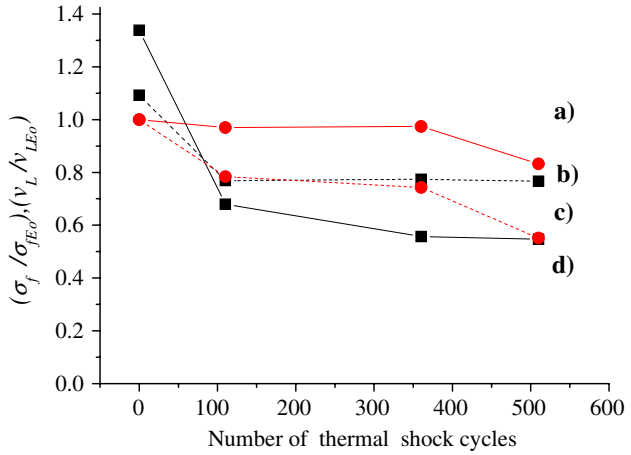

Fig. 2 Fracture strength and ultrasonic velocity through the thickness as function of number of thermal-shock cycles, where the curves labeled (a) corresponds to σ_f of BRT, (b) v_L of RSE samples, (c) v_L of BRT and (d) σ_f of RSE material, respectively. The average relative standard deviation is less than 5%

The values are given relative to the values of fracture strength and ultrasonic velocity measured on as-received samples (σ_{E0} and v_{LE0}). It is evident observing Fig. 2 that the fracture strength of RSE material is higher than that of BRT in the as-received condition. The strength of both materials decreases initially rapidly, in particular for RSE material, and after about 100 thermal-shock cycles the values tend to saturation with increasing number of cycles.

Figure 2 also shows a remarkable similarity between the trends of σ_f and v_L, as can be observed comparing the curves labeled (a)–(c) and (b)–(d); where curves (a) and (c) correspond to σ and v_L of BRT material; while (b) and (d) curves to RSE material, respectively. This fact can be explained considering the Griffith theory [25]. In a previous investigation it was demonstrated that the on-duty fracture of these refractory plates can be correlated to a single dominant phenomena with a major crack aligned in parallel to the transversal direction of the sample [13]. The suitable set-up of the UPV transducers during the measurement of v_L permitted the detection of the onset of crack initiation and the progress of further microcracking development into macroscopic damage. The critical length sizes were found to be ~700 μm and ~500 μm for BRT and RSE refractory plates, respectively (results not shown here). Longer cracks will propagate at higher crack-growth rates, as demonstrated in Ref. [26]. In many of the investigated samples, cracks are already visible after approximately 100 cycles, with crack lengths higher than 1 mm [13]. Table 3 summarizes the fitting equations of thermo-mechanical properties for industrial thermal-shock cycles (corresponding to the data in Fig. 2), including correlation coefficients and standard deviations.

The retained strength (Eq. 8) after 110 cycles is 90% for BRT material while RSE material retains only 70% as reported in Table 3. When the number of cycles is 360, the retained strength of the refractory materials remains almost constant, about 90% for BRT and 70 % for RSE, respectively. The higher retained strength of BRT material indicates that it should behave better under thermal-shock conditions. In fact from the 50 refractory plates studied of each composition, 13 plates of BRT material survived 510 cycles without visible fractures, while for RSE material the number of undamaged plates was only 5. Such damage of RSE material could be induced by stresses arising from

Table 3 Equations of thermo-mechanical property variation with thermal-shock cycles, including correlation coefficients, relative standard deviation and retained property values

Parameter (Y)		Fitting equations 1st, 2nd, 3rd order exponential decays fitting constants: y0, A1, t1, A2, t2, A3, t3		Correlation coefficient (R^2)		Average relative standard deviation (%)		Retained property ratio after 100 cycles (%)	
		RSE	BRT	RSE	BRT	RSE	BRT	RSE	BRT
Three point bending strength σ (MPa)		$y = yo + A1 * e^{\frac{-x}{t1}} + A2 * e^{\frac{-x}{t2}} + A3 * e^{\frac{-x}{t3}}$	$y = yo + A1 * e^{\frac{-x}{t1}}$	0.98	0.97	6	5	70	90
Fracture toughness K_{IC} (MPa $m^{1/2}$)		$y = yo + A1 * e^{\frac{-x}{t1}}$	$y = yo + A1 * e^{\frac{-x}{t1}} + A2 * e^{\frac{-x}{t2}}$	0.92	0.92	15	14	67	79
Ultrasonic velocity v (m/s)	v_L	$y = yo + A1 * e^{\frac{-x}{t1}} + A2 * e^{\frac{-x}{t2}} + A3 * e^{\frac{-x}{t3}}$	$y = yo + A1 * e^{\frac{-x}{t1}} + A2 * e^{\frac{-x}{t2}}$	0.99	0.9	19	19	51	78
	v_T	$y = yo + A1 * e^{\frac{-x}{t1}} + A2 * e^{\frac{-x}{t2}} + A3 * e^{\frac{-x}{t3}}$	$y = yo + A1 * e^{\frac{-x}{t1}}$	0.99	0.5	5	5	88	99
Damage surface P_0/P (%)		$y = yo + A1 * e^{\frac{-x}{t1}}$	$y = yo + A1 * e^{\frac{-x}{t1}} + A2 * e^{\frac{-x}{t2}}$	0.99	0.97	–	–	98	92
R (°C)		$y = yo + A1 * e^{\frac{-x}{t1}}$	$y = yo + A1 * e^{\frac{-x}{t1}} + A2 * e^{\frac{-x}{t2}}$	0.87	0.94	19	19	68	160
R'''' (m)		$y = yo + A1 * e^{\frac{-x}{t1}} + A2 * e^{\frac{-x}{t2}}$	$y = yo + A1 * e^{\frac{-x}{t1}}$	0.87	0.91	15	14	89	65
$\frac{d\sigma_f}{dE_{dyn}}$		$y = yo + A1 * e^{\frac{-x}{t1}}$	$y = yo + A1 * e^{\frac{-x}{t1}}$	0.87	0.86	–	–	88	534

thermal expansion mismatch between the coarse grain aggregates (molochite, fused silica, etc.) and the cordieritic matrix (see microstructure image, Fig. 1b). Thermal expansion anisotropy of the aggregate grains and stresses from the non-linear temperature distribution present during the thermal cycles, as explained in previous investigations [17, 18], should also contribute to the observed different behavior of the materials.

Fracture toughness-surface damage parameter correlation

Figure 3a shows the variation of K_{IC} and surface damage parameter ($\frac{P_0}{P}\%$) with industrial thermal-shock cycles. The values are given relative to the fracture toughness and damage surface of as-received BRT samples. It is evident that BRT presents higher values of K_{IC} and $\frac{P_0}{P}\%$ than RSE material during all their service life. Likewise there is a clear significant correspondence between the trends of K_{IC} and $\frac{P_0}{P}\%$ for both materials. This could be due to the capability of image analysis to monitor the development of surface degradation, which is strongly related to the quality of the interface between mullitic aggregate grains and the cordieritic-matrix. Thermal-shock cycles induce change in the microstructure and thermal aging effects, leading to weakening of this interface and as consequence grains can be removed easier. Optical micrographs of fracture surfaces obtained on thermally shocked samples (110 cycles) after fracture toughness test confirmed the presence of grain pull-out effects in both compositions, but in particular with higher frequency in RSE composites, as Fig. 4a, b demonstrates. The more detailed analysis of fracture morphology has been presented elsewhere [27, 28]. When the specimens were covered with thin chalk-powder film, the grain pull-out effect was also evident from the optical microscopy images used for $\frac{P_0}{P}\%$ ratio assessment, reported in Fig. 5a, b. The higher fracture toughness values of BRT material (Fig. 3b) can be mainly attributed to the presence of silicate glassy phases at the mullitic-aggregates/cordieritic-matrix interface and to the higher amount of cordieritic matrix in comparison to RSE material, leading to a major presence of viscoelastic crack bridging phenomena, as can be seen in the micrographs shown in Fig. 1a, b (black arrows indicate possible crack bridges). Indeed, it can be inferred observing Fig. 1a, b, that BRT

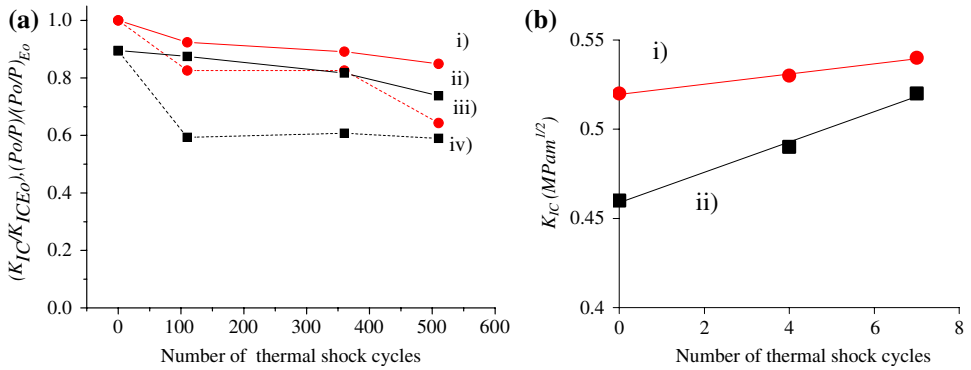

Fig. 3 (**a**) Fracture toughness, K_{IC}, and damage surface values ($\frac{P_0}{P}\%$) against number of thermal-shock cycles. The curves labeled (i) corresponds to K_{IC} of BRT, (ii) K_{IC} of RSE samples, (iii) ($\frac{P_0}{P}\%$) of BRT and (iv) ($\frac{P_0}{P}\%$) of RSE material, respectively. (**b**) Enlargement of absolute values of K_{IC} in the 0–7 thermal-shock range determined by the chevron-notched technique for (i) BRT and (ii) RSE samples. The average relative standard deviation is less than 15%

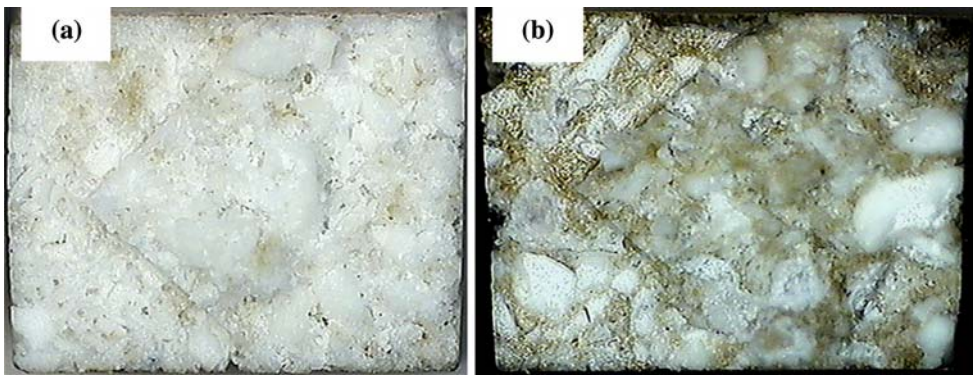

Fig. 4 Optical microscopy micrographs of fracture surfaces of chevron notched samples after 110 thermal-shock cycles: (**a**) BRT and (**b**) RSE samples

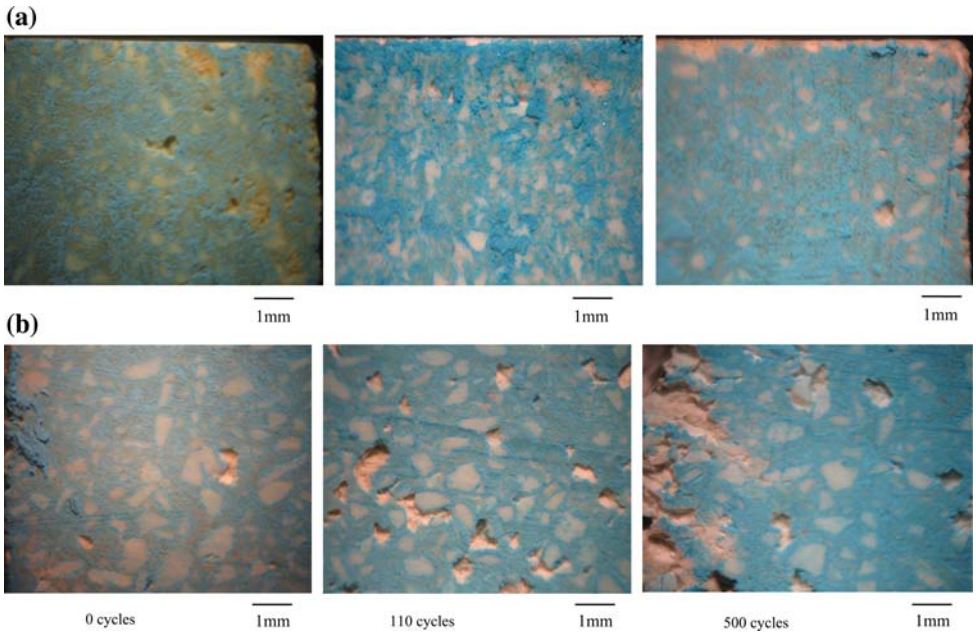

Fig. 5 Images of surface degradation for samples before and after 110 and 510 thermal-shock cycles for (**a**) BRT and (**b**) RSE refractory materials

apparently presents more microstructural bridges between chamotte grains and cordieritic matrix (black arrows) than RSE material, and presumably as consequence a major viscoelastic bridging effect could be expected. The effect of microstructure on fracture toughness has been investigated elsewhere [17]. Briefly, the presence of this cordieritic glassy matrix is thought to be responsible for crack blunting, shielding and crack bridging, while the silicate glassy phases in the grain-matrix interface can lead to a crack branching toughening mechanism. It is thought that these toughening mechanisms can play a more dominant role in the improvement of fracture toughness than the probably decrease of K_{IC} caused by the diminution of crack deflection due to the higher amount of glassy phase. In addition, the smaller size of mullitic aggregates in BRT material leads to better thermo-mechanical properties including lower thermal expansion coefficient [18].

An unexpected increasing trend of K_{IC} values for both refractory compositions was found in the first 7 cycles, in particular for RSE material, as Fig. 3b depicts. Optical stereomicroscopy of fracture surfaces has shown that in both materials the major changes upon thermal-shock loading occurred on boundaries between crystalline phases forming the refractory composite microstructure. Due to grain boundary embrittlement at the mullitic aggregate/cordieritic matrix interface, more intergranular microcracking was observed with increasing number of thermal-shock cycles. The increase in fracture toughness of RSE samples after seven thermal-shock cycles could be assigned to a crack shielding effect at grain boundaries [27]. A complete description of toughening mechanisms possibly acting in cordierite–mullite refractories as function of the raw materials employed (chemical composition, chamotte amount, etc.) is described elsewhere [22], and it is the focus of a current investigation. Briefly, it has been observed that the use of fused silica in the grog batch can promote the development of multilayer glassy phases surrounding these fused silica grains. The evolution of these glassy phases with temperature indicates that at elevated temperature the glass becomes viscous and a crack blunting toughening mechanism could be expected. On cooling after thermal shock, this glass could induce crack branching and crack shielding effects on the propagating cracks improving the overall fracture toughness property of the material. This effect should be high in the coarse grained material (RSE) (Figs. 1b, 4b) whereas for the fine grained material (BRT) (Figs. 1a, 4a) the effect should be negligible. This explains the fact that for both materials the decreasing trend of K_{IC} begins after 10–15 cycles when the development of crack shielding effects at grain boundaries has been completed, as shown elsewhere [18]. After 15 industrial thermal cycles, the fracture toughness trend of BRT material is less pronounced than for RSE, suggesting again that BRT is less sensitive to damage under repeated thermal shocks than RSE material. From an industrial point of view a reliable parameter is desired, which could be used to extrapolate the long-term behavior of the material after testing for only few cycles. It seems that the $\frac{\sigma_r}{\sigma_o}$ ratio is more suitable than $\frac{K_{IC}}{K_{IC_o}}$ ratio since the former does not present the initial increasing trend, hence after a fewer number of initial cycles the thermal-shock behavior can be predicted.

Optical micrographs of refractory surfaces subjected to increasing number of thermal-shock cycles are shown in Fig. 5. The analysis of a relevant number of micrographs by means of Image Pro Plus software permitted the

determination of the surface damage parameter $(\frac{P_0}{P}\%)$ accurately.

Table 3 reports the service life equations obtained by fitting the average values of the $(\frac{P_0}{P}\%)$ ratio by an exponential function, which shows very high-correlation coefficients (0.99 and 0.97 for RSE and BRT samples, respectively).

Correlation between Hasselman's parameters R, R'''' and microstructure. The variation of $\frac{d\sigma_f}{dE_{dyn}}$ as a new approach for characterization of thermal-shock damage

Figure 6a illustrates the variation of the parameter "R" with the number of thermal cycles. As mentioned above, the primary effect of thermally cycling refractory materials is the development of microcracks. According to Hasselman's theory [29] crack amount, orientation and their interaction play a significant role in defining the effect of microcracks on mechanical behavior. While there has been extensive research linking mechanical properties and porosity, much less work has focused on the effect of microcracks on mechanical properties [30]. One of the most commonly used equations describing the effect of porosity on elastic properties is the exponential function [29–31]:

$$X = X_0 * e^{(-\alpha V)} \tag{9}$$

where X is the elastic property of the dense material, V the volume fraction of porosity and α a constant determined by the Poisson's ratio as well as pore shape and orientation.

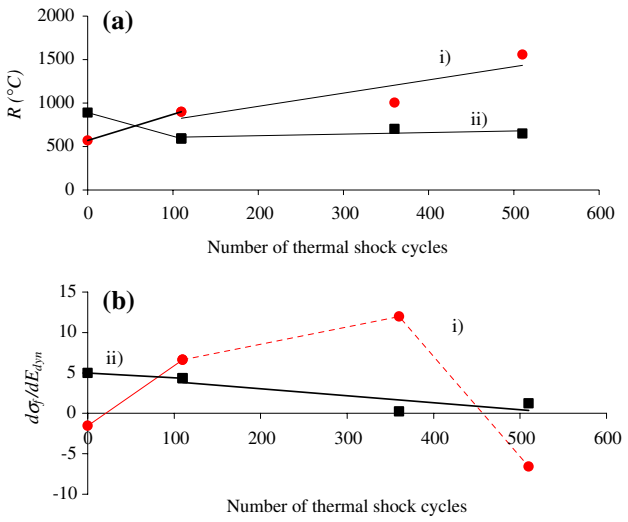

Fig. 6 (**a**) Calculated fracture resistance parameter (R) as function of thermal-shock cycles for (i) BRT and (ii) RSE samples. The average relative standard deviation is less than 20%; (**b**) $\frac{d\sigma_f}{dE_{dyn}}$ trend with number of cycles for (i) BRT and (ii) RSE samples (lines are drawn for eye help only)

The equation could also be applied for predicting the effect of microcraks on elastic constants. This equation indicates that with an increase in porosity/microcracks fraction in the body, the decrease in elastic properties values can be understood as the effect of adding a second-phase of zero elastic modulus. This equation should also describe the variation of fracture strength when the cracks present in the material do not go beyond the critical length value and the ratio between elastic and mechanical properties is governed by the Hooke's law. When the defects present in the material are longer than the critical length, cracks will propagate faster and further thermal cycling will inevitably reduce the fracture strength by a different decreasing law than that expressed by Eq. 9. The factors controlling the resistance to fracture initiation of refractory materials under thermal-shock conditions or thermal stress resistance, as expressed by the R parameter, are well known [29] and for cases where crack interaction can be ignored a quantitative analysis is possible. However, at high microcrack concentration, where the distance between cracks is of the order of the crack dimension, crack interaction effects are likely to become relevant and a full analysis of their influence on modulus and strength is more problematic. The resistance to fracture initiation of refractory materials, which is quantified by the parameter R, is mostly related to the $\frac{\sigma_f}{E}$ ratio, as Eq. 5 shows, assuming no significant variations of thermal expansion coefficient with thermal cycling. In many materials containing high densities of microcracks the effect of microcracking appears to be greater on modulus than on strength, and the strength/modulus ratio is higher compared to that of the uncracked material, with consequent increases in R. In these materials cracks and voids act as a second phase of zero modulus and this can be considered the dominant effect for the increasing behavior of R with thermal cycling [32]. Instead, for materials exhibiting decreasing R behavior, strength reduction diminution is the dominant effect. This means that the rate of interconnection between cracks with successive thermal-shock cycles can lead to cracks longer than the critical length, and the rate of propagation of this effect in the material microstructure with increasing thermal-shock cycles is higher than the decrease of dynamic Young's modulus due to the increasing presence of cracks with zero elastic modulus.

In our study the thermal-shock resistance parameter (R) was calculated using Eqs. 4 and 6, where E_{dyn} is the dynamic Young's modulus and v the ultrasonic velocity measured through the thickness path (v_T) of the refractory plates. It was assumed that α would not substantially change with thermal-shock cycles, based on literature results [33]. v_T was selected for the determination of dynamic Young's modulus (E_{dyn}) because the variations of v_T (and three point bending strength (σ_f)) with thermal

cycling are closely related to microcracking due to thermal aging effects, as demonstrated in a previous work [13]. On the other hand, the variation of v_L with thermal cycling is related to the presence of critical macro-cracks that, propagating in the transversal direction, can cause the refractory plate fracture. It was found that BRT material presents a dynamic Young's modulus dominant effect on R behavior and hence the rate of interconnection between cracks with number of thermal shock cycles should be lower than the rate of decrease of elastic modulus. On the other hand, the RSE material showed a fracture strength dominant effect and hence the crack propagation should play the major role.

Figure 6a shows that BRT material has a lower value of R in the as-received state, which means a lower resistance to fracture initiation under thermal shock. However, this material presents an increasing trend of this parameter with number of cycles during almost its entire service life, which clearly indicates a better resistance to further crack propagation (as explained above, this behavior indicates lower velocity of crack propagation than the rate of elastic modulus decrease). The RSE material presents a higher value of resistance R from the as-received conditions up to approximately 50 cycles. This behavior corresponds to the fact that this material shows a delayed fracture initiation with regard to BRT material, according to industrial data available [17]. However, the R-value decreases further with the number of thermal cycles and this indicates a high velocity of crack propagation. Figure 6b reports the variation of $\frac{d\sigma_f}{dE_{dyn}}$ with number of cycles. It is noticeable the sensitivity that this ratio possesses to determine changes in the material induced by thermal-shock cycles, which is manifested by the high gradient obtained in the trend after 110 cycles (see also Table 3). Observing Fig. 6b, a high and positive value of $\frac{d\sigma_f}{dE_{dyn}}$ gradient for BRT material is apparent after 110 cycles while for RSE material it is possible to observe a slight decrease of $\frac{d\sigma_f}{dE_{dyn}}$ with the number of cycles. This appreciable difference suggests the convenient use of this parameter to distinguish refractory materials regarding their different thermal-shock behavior and its use to predict service life performance of different refractory materials.

Examination of SEM micrographs of materials in the as-received state indicate that they were extensively micro-cracked and cracks were predominantly intergranular (see white arrows in Fig. 1a, b). Figure 7a, b shows SEM images of the matrix microstructure of the refractory materials investigated, while Fig. 7c, d report the porosity of the mullitic aggregates in as-received condition. Although both materials present random orientation of these pre-existing cracks, the BRT material shows smaller pore sizes for both matrix and grain microstructure. The crack amount and morphology can be quantitatively characterized by the statistical determination of the roundness parameter by means of image analysis [34]. This could lead to lower rate of interconnection between cracks with number of cycles thus explaining the increasing R behavior of BRT material. SEM micrographs of the microstructure of samples after 110 cycles show that for both materials the major cracking event might be better described as aggregate–matrix bond interface separation, as can be seen in Fig. 1c, d. In the cordierite–mullite composites examined in this work, it is thought that the interaction between aggregate–matrix bond interface cracks and matrix flaws is the effect playing a major role on the mechanical properties. The mean distance between aggregate–matrix bond interface cracks was determined by image analysis measurement on a representative number of microstructure micrographs. The measured mean values of the distance between cracks are of the order of the crack length and approximately equivalent to the aggregate grain dimension, being 600μm for RSE and 450μm for BRT materials, respectively. Indeed, as Fig. 1b, d shows, the larger aggregate grains of RSE material appear to have a significant function of providing the connectivity between cracks.

Figure 8 shows the trend of thermal-shock resistance parameter R'''' with thermal-shock cycles, calculated by Eq. 7 and using the ultrasonic velocity values measured through the thickness path (v_T). Clearly, crack stopping is an extremely important process in refractory structures; for unless crack arrest occurs, there will be catastrophic failure every time that thermal-shock damage is initiated. Considering Eq. 7 it is evident that a decreasing R'''' behavior with thermal-shock cycles can be only explained if the rate of degradation of K_{IC} is higher than that of σ_f. BRT materials present a higher value of R'''' in the as-received state, which indicates higher resistance to propagation of the pre-existing cracks. R'''' decreases drastically during the first 100 cycles for both materials and then a relatively constant value similar for both refractories is reached. In particular, it can be observed that the decrease of R'''' for the BRT refractory material is more severe than that for RSE material. This can be mainly attributed to the deterioration of the toughening mechanisms active in the BRT refractory microstructure due to thermal aging effects. Nevertheless, R'''' of BRT material is higher than that of RSE material during all their service life (up to 500 cycles).

Table 3 summarizes the results of the measurements of the thermo-mechanical properties of as-received and thermally cycled samples and the fitted equations, including correlation coefficients and standard deviation values. From the analysis of the retained property ratios an assessment about which parameter could be used to predict thermal-shock behavior during service life can be made. The retained values of all investigated thermo-mechanical

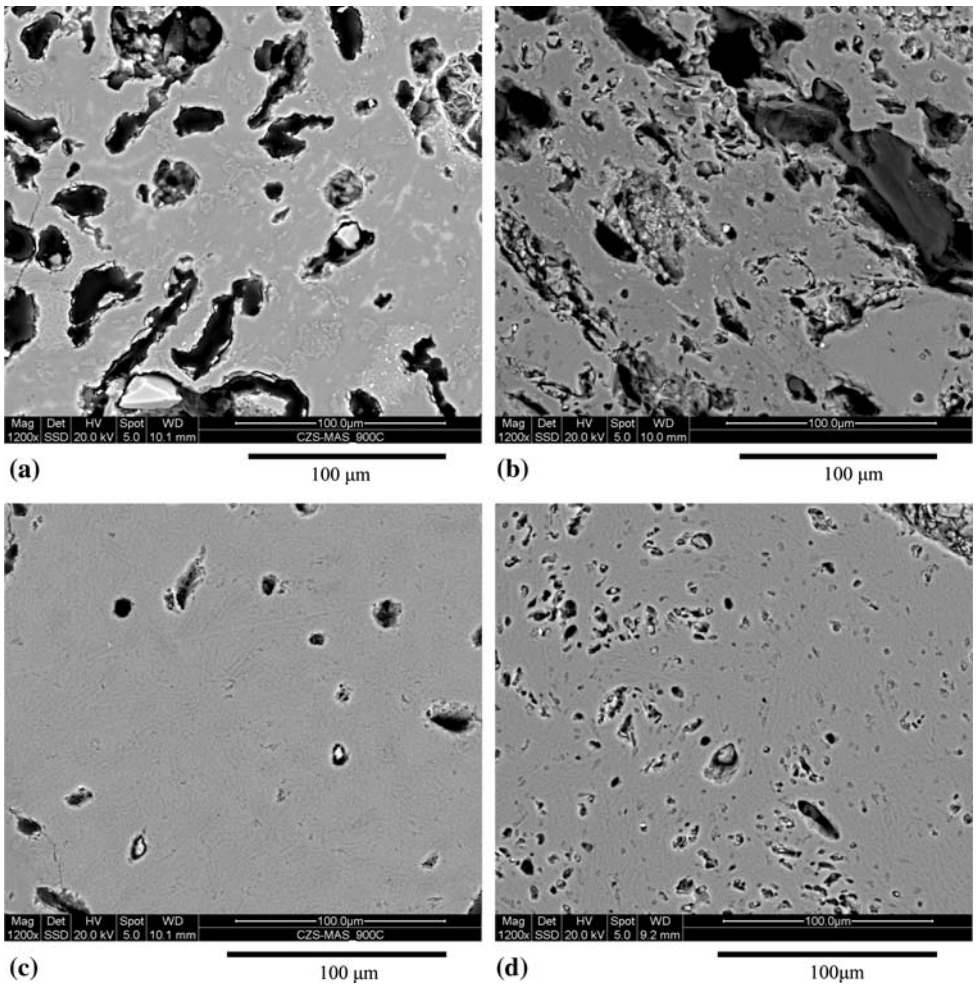

Fig. 7 SEM micrographs of as received samples where (**a**) and (**b**) correspond to cordierite matrix of BRT and RSE samples, respectively, and (**c**) and (**d**) correspond to aggregate microstructures of BRT and RSE samples, respectively

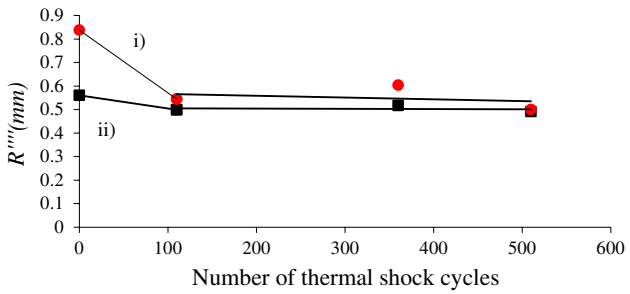

Fig. 8 Calculated R'''' parameter against number of thermal-shock cycles for (i) BRT, (ii) RSE materials, respectively (lines are drawn for eye help only). The average relative standard deviation is 15 %

properties as well as image analysis and ultrasonic velocity measurements coincide in the assessment that the BRT material exhibits better resistance to thermal shock, as discussed in detail above in section "Results and discussion". This suggests that non-destructive testing, like image analysis and UPVT measurement, can be used to find reliable empirical correlations for prediction of service life of materials under thermal-shock conditions. In particular, it was found that the $\frac{d\sigma_f}{dE_{dyn}}$ ratio shows the highest gradient of retained property and therefore of sensitivity to assess thermal-shock damage.

Conclusions

The thermal-shock resistance of two refractory materials was investigated by destructive tests (fracture strength and fracture toughness) measurements and non-destructive examination (ultrasonic pulse velocity testing and image analysis). A remarkable similarity was found between the variations of ultrasonic velocity (when measured through the length of the refractory plates) and fracture strength with number of thermal-shock cycles. It is thought that this is related to the suitable setting of the UPVT transducers, which are able to detect the development and propagation of critical cracks from the micro to the macro-structure level in the transversal direction; cracks that ultimately lead the investigated refractory plates to fracture. On the other hand, the development of surface microcracking, as monitored by image analysis, is in good agreement with the variation of K_{IC} with the number of thermal shock cycles.

A possible explanation for this good fitting could be the high dependence of fracture toughness values on the quality of the aggregate–matrix bond interface and grain pull-out effect; and the high capability of the software used for image analysis to detect the increasing extent of grain-pull-out due to thermal degradation of the refractory microstructure.

A constant *R*-value for increasing number of thermal-shock cycles should be set as the lowest threshold behavior in the refractory material design. This ensures a low rate of material degradation equivalent to the rate of decrease of dynamic Young' modulus with number of thermal cycles. Materials with increasing trend of *R* versus number of thermal-shock cycles will present even lower velocities of crack propagation than the rate of elastic modulus degradation.

A better thermal-shock resistance was found for the BRT material. This material exhibits a favorable combination of thermo-mechanical properties and microstructure features leading to an overall optimized behavior under thermal shock. All destructive and non-destructive characterization tests performed in this work converge in this assessment. The variation of the $\frac{d\sigma_f}{dE_{dyn}}$ ratio with number of thermal-shock cycles shows the highest gradient of the investigated trends and it is proposed as a promising parameter to differentiate refractory materials regarding their different thermal-shock behavior.

Finally, it was shown that UPVT and image analysis can characterize effectively the thermal stability of refractory materials and semi-empirical mathematical models are proposed to predict service life of refractory materials under cyclic thermal shock.

Acknowledgement Financial support provided by the Czech Science Foundation under projects number 106/05/0495 is gratefully acknowledged.

References

1. Aneziris CG, Klippel U, Schärfl W, Stein V, Li Y (2007) Int J Appl Ceram Techn 4(6):481
2. Baker TJ, Zimba J, Akpan ET, Bashir I, Watola CT, Soboyejo WO (2006) Acta Mater 54:2665
3. Bolelli G, Cannillo V, Lugli C, Lusvarghi L, Manfredini T (2006) J Eur Ceram Soc 26:2561
4. Norton FH (1931) In: Refractories. Mcgraw-Hill, New York, 3rd edn., 1949
5. Goodrich HR (1927) J Am Ceram Soc 10:784
6. Hasselman DPH (1969) J Am Ceram Soc 52:600
7. Hasselman DPH (1970) Bull Am Ceram Soc 49:1033
8. Nakayama J (1964) Jpn J Appl Phys 3:422
9. Davidge RW, Tappin G (1967) Trans Br Ceram Soc 66:405
10. Tacrarian MS (1955) Bull Soc Fr Ceram 29:20
11. Fawzy A, Charles ES (1985) Am Ceram Soc Bull 64:1555
12. Lawlar JG, Ross RH, Rub E (1981) Am Ceram Soc Bull 60:713
13. Boccaccini DN, Romagnoli M, Kamseu E, Veronesi P, Leonelli C, Pellacani GC (2007) J Eur Ceram Soc 27:1859
14. Nyiogi SK, Das AC (1994) Interceram 43:453
15. Volkov-Husovic TD, Majstorovic J, Cvetkovic M (2003) Interceram 52:296
16. Volkov-Husoviæ TD, Janèiæ RM, Mitrakoviæ D (2005) Am Ceram Soc Bull 84:1
17. Boccaccini DN, Leonelli C, Rivasi MR, Romagnoli M, Boccaccini AR (2005) Ceram Int 31:417
18. Leonelli C, Boccaccini DN, Dlouhy I, Veronesi P, Cannillo V, Boccaccini AR (2007) Adv Appl Ceram 106:142
19. Boccaccini AR, Rawlings RD, Dlouhy I (2003) Mater Sci Eng A 347:102
20. Bluhm JI (1975) Engng Fract Mech 7:593
21. Pickles CSJ, Field JE (1996) J Phys D: Appl Phys 29:436
22. Boccaccini DN (2007) Study of thermal conductivity in refractory materials by means of a guarded hot plate apparatus, in study of thermomechanical properties of refractory materials by non-destructive methods, design of facilities for thermomechanical properties characterization, PhD Thesis, University of Modena and Reggio Emilia. Dip. Ing. Mat. e dell'Ambiente
23. Emery AF (1980) In: Hasselman DPH, Heiler RA (eds) Thermal stresses in severe environment. Plenum Press, New York
24. Boccaccini AR, Ponton CB, Chawla KK (1998) Mat Sci Eng A 241:141
25. Gdoutos EE (1993) In fracture mechanics: an introduction. Kluwer Academic Publishers, Dordrecht
26. Boccaccini DN, Volkov Husovic T, Romagnoli M, Veronesi P, Cannio M, Leonelli C, Pellacani G, Boccaccini AR (2007) Int J Appl Ceram Tec 4(3):260
27. Chlup Z, Dlouhy I, Boccaccini AR, Boccaccini DN, Leonelli C, Romagnoli M (2005) Key Eng Mater 290:260
28. Chlup Z, Boccaccini D, Leonelli C, Romagnoli M, Boccaccini AR (2006) Silikáty 50:245
29. Hasselman DPH, Singh JP (1979) Am Ceram Soc Bull 58:856
30. Rice RW (1998) In: Porosity of ceramics. Marcel Dekker, New York, p 539
31. Ryshkewitch E (1953) J Am Ceram Soc 36:65
32. Boccaccini AR, Ondracek G, Mazilu P, Windelberg D (1993) In: Duran P, Fernandez JF (eds) On the porosity dependence of the fracture strength of ceramics in third Euro-ceramics, engineering ceramics, vol 3, p 895
33. Davis WR (1968) Trans Brit Ceram Soc 67:515
34. Baxes GA (1994) Digital image processing principle and applications. John Wiley and sons Inc, New York, p 157